

Acoustic Partial Discharge Localization in Refined, Bleached and Deodorized Palm Oil (RBDPO) Based on the Savitzky-Golay and Moving Average Denoising Methods

Nur Darina Ahmad^{1,2}, Norhafiz Azis^{1*}, Jasronita Jasni¹, Khairil Anas Md Rezali³, Mohd Aizam Talib⁴, Nik Hakimi Nik Ali⁵ and Masahiro Kozako⁶

¹*Advanced Lightning, Power and Energy Research Centre (ALPER), Department of Electrical and Electronics Engineering, Universiti Putra Malaysia, 43400 UPM Serdang, Selangor, Malaysia*

²*Electrical Engineering Studies, College of Engineering, Universiti Teknologi MARA, Pulau Pinang Branch, 13500 Permatang Pauh, Pulau Pinang, Malaysia*

³*Department of Mechanical and Manufacturing Engineering, Faculty of Engineering, Universiti Putra Malaysia, 43400 UPM Serdang, Selangor, Malaysia*

⁴*Advanced Diagnostic Services, TNB Labs Sdn Bhd, 43000 Kajang, Selangor, Malaysia*

⁵*School of Electrical Engineering, College of Engineering, Universiti Teknologi MARA (UiTM), 40450 Shah Alam, Selangor, Malaysia*

⁶*Department of Electrical and Electronic Engineering, Kyushu Institute of Technology, Kitakyushu-shi, Fukuoka, Japan*

ABSTRACT

This research describes an investigation on the localization of partial discharge (PD) in Refined, Bleached and Deodorized Palm Oil (RBDPO) with the applications of 2 denoising methods, namely Savitzky-Golay (SG) and Moving Average (MA). A needle-plane electrode setup was used to initiate the PD. The electrical PD signal measurement was carried out through the impedance matching circuit (IMC), and the acoustic PD signal was obtained by acoustic emission (AE) sensors. The AE sensors were attached to the tank's surface, and pre-amplifiers were used to boost the acquired

acoustic PD signal. A high-voltage AC supply initiated the PD within the test tank filled with RBDPO. Both electrical and acoustic PD signals were denoised by SG and MA methods. The 2 denoising methods were evaluated based on the signal-to-noise ratio (SNR), root mean squared error (RMSE) and correlation coefficient (CC) metrics. The denoised acoustic PD signals were then utilized in the time difference of arrival (TDOA) technique to perform PD localization. The SG was found to be more effective than the MA in denoising both the electrical and acoustic

ARTICLE INFO

Article history:

Received: 01 April 2024

Accepted: 10 April 2025

Published: 10 June 2025

DOI: <https://doi.org/10.47836/pjst.33.S4.07>

E-mail address:

nurdarina9183@uitm.edu.my (Nur Darina Ahmad)

norhafiz@upm.edu.my (Norhafiz Azis)

jas@upm.edu.my (Jasronita Jasni)

khairilanas@upm.edu.my (Khairil Anas Md Rezali)

aizam.talib@tnb.com.my (Mohd Aizam Talib)

hakimial@uitm.edu.my (Nik Hakimi Nik Ali)

kozako@ele.kyutech.ac.jp (Masahiro Kozako)

*Corresponding author

PD signals based on its low RMSE and high CC. The estimated PD source locations based on the SG-denoised acoustic PD signals are closer to the actual PD source than those derived from the MA-denoised signals.

Keywords: Acoustic partial discharge, moving average (MA), partial discharge localization, RBDPO (refined, bleach and deodorized palm oil), Savitzky-Golay (SG), time difference of arrival (TDOA)

INTRODUCTION

Partial discharge (PD) is a phenomenon that can affect the insulation in transformers. PD diagnostic is commonly employed due to its high sensitivity (Firuzi et al., 2019). Localization of PD can further be used to pinpoint the location of potential problems in the insulation system (Karami et al., 2020). Furthermore, it can help with the targeted maintenance scheme of transformers (Chan et al., 2023; Zhang et al., 2018).

The introduction of Refined, Bleached and Deodorized Palm Oil (RBDPO) as a possible substitute for mineral oil in transformers promotes sustainable initiatives in industries (Rafiq et al., 2015). Several studies have examined the suitability of RBDPO for this purpose (Azis et al., 2014; Mustam et al., 2023). Currently, the study related to acoustic PD source localization in RBDPO is still limited.

It is known that PD could be identified through electrical, chemical, acoustic and electromagnetic approaches. Acoustic PD signal often consists of both PD signal and noise components, necessitating denoising techniques to enhance detection accuracy (Hussain et al., 2021). The Savitzky-Golay (SG) is known as one of the denoising methods used in different types of applications, such as acoustic PD source localization in mineral oil, medical electromyography signal, on-load tap changer vibro-acoustic signal and sulfur hexafluoride corona discharge data (Dombi & Dineva, 2020; Feizifar et al., 2019; Li et al., 2021; Lonkwic et al., 2017; Seo, 2018a, 2018b; Yang et al., 2022). Moving Average (MA) is applied for electrical and acoustic PD source localization in mineral oil, communication echo signal/temperature data and photochemical and electrochemical reactor data (Ghosh et al., 2017; Guiñón et al., 2007; Hashim et al., 2023; Purnamasari et al., 2021). SG and MA methods are widely used in various applications due to their simplicity, efficiency and ability to preserve important signal features while reducing noise.

This study investigates the localization of the estimated PD source in RBDPO based on the electrical and acoustic PD signals denoised by SG and MA methods. These PD signals are acquired through an impedance matching circuit (IMC) and acoustic emission (AE) sensors. The acoustic PD source localization is based on the time difference of arrival (TDOA) outputs determined from the denoised acoustic PD signals. The performances of denoising methods are analyzed through signal-to-noise ratio (SNR), root mean squared

error (RMSE) and correlation coefficient (CC) metrics. The accuracy of the acoustic PD source localization is examined through location error analysis.

MATERIALS AND METHODS

Oil Preparation

Refined, Bleached and Deodorized Palm Oil (RBDPO) was used in this study, whereby the properties can be seen in Azis et al. (2014). The RBDPO was first subjected to filtration with a $0.22\ \mu\text{m}$ membrane filter. After filtration, the RBDPO was dried in an air-circulating oven at $85\ ^\circ\text{C}$ for 72 hours.

Experiment Setup

A steel test tank with dimensions of 40 cm in length, 25 cm in width, 25 cm in height and a maximum capacity of 20 liters was employed for the experiment. PD was produced through a needle-plane electrode setup with a gap distance between the needle tip and the surface of the plane electrode fixed at 50 mm throughout the experiment. The needle has a tip radius of $3\ \mu\text{m}$, and the diameter of the plane ground electrode is 50 mm. Figure 1 depicts the test circuit for electrical and acoustic PD measurement, whereby the measurement is carried out in accordance with IEC 61294 and IEC 60270 (Fuhr, 2005; Pattanadech & Muhr, 2017). Figure 2 illustrates an example of the AE sensors and needle-plane electrode placements. A 3D coordinate system was established for the steel tank, whereby one of the bottom corners of the tank was set as the origin (0, 0, 0) m, as shown in Figure 3. Based on this coordinate system, the actual PD source was set at (0.07, 0.08, 0.18) m.

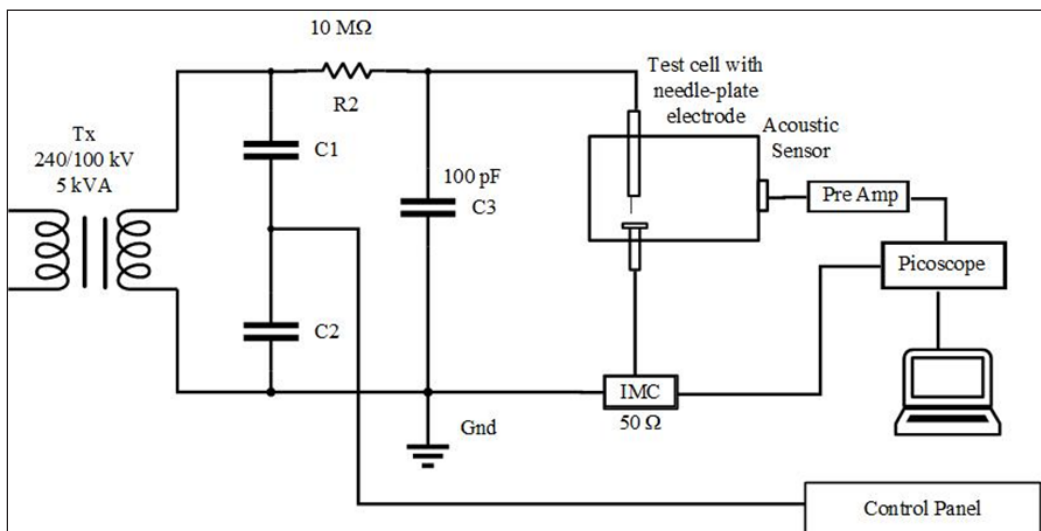


Figure 1. Experimental configuration for electrical and acoustic partial discharge measurements

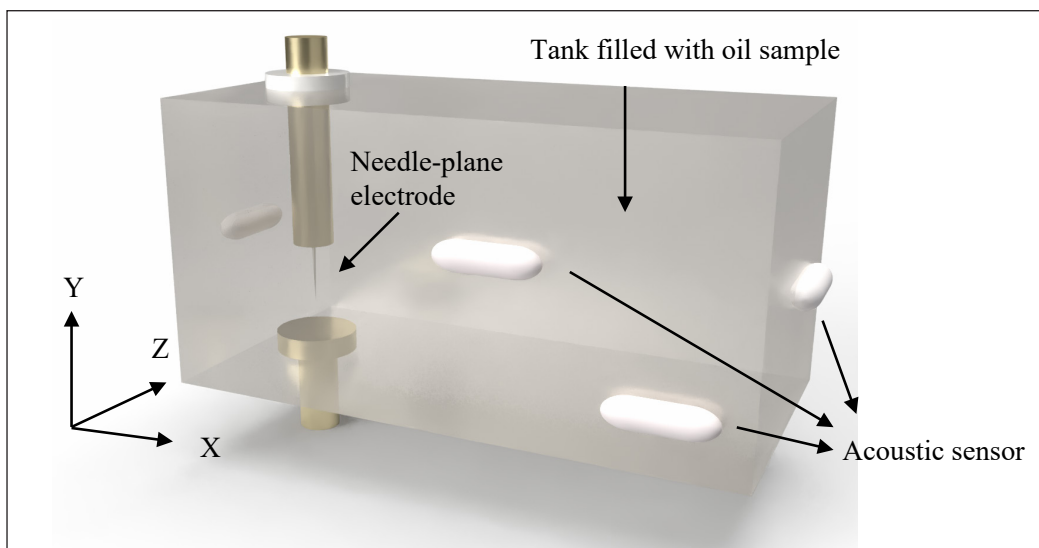


Figure 2. Example of needle-plane electrodes and acoustic emission sensor placements

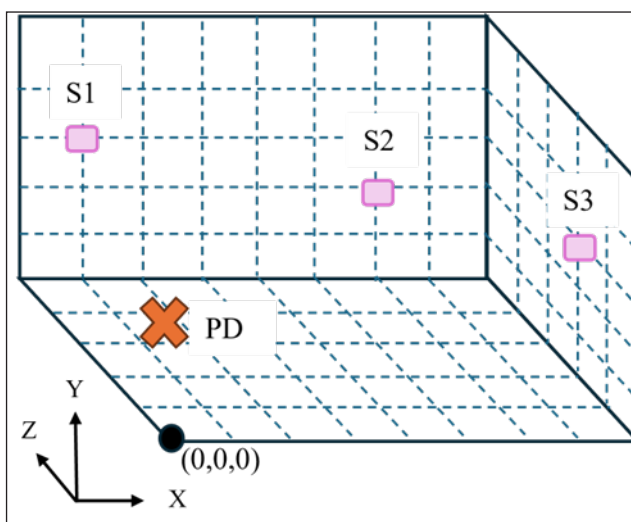


Figure 3. Coordinate marking for partial discharge localization

A high-voltage AC supply with a rating up to 100 kV was utilized to supply the voltage at the needle electrode, as shown in Figure 1. The supply voltage was increased at a constant step of 5 kV from 15 kV to 40 kV. In this study, 4 AE sensors were applied to capture the acoustic PD signals, as depicted in Figure 3. The operating frequency range of these AE sensors is between 20 and 180 kHz. Each AE sensor was connected to a pre-amplifier with 60 dB gain. The sensitivity of the AE sensor was checked based on IEEE C.57.127 (Ghosh et al., 2017). The electrical PD signal was acquired via an IMC with input and

output impedances of 50Ω respectively. The acoustic PD signals were collected once the electrical PD signals exceeded the partial discharge inception voltage (PDIV), which ranges from 120 pC to 140 pC, depending on the surrounding noise and weather. PicoScope 4824 with a sampling frequency up to 80 MS/s was used to acquire the electrical and acoustic PD signals simultaneously.

Acoustic Emission Sensors Positioning

Sixty-four different combinations of AE sensors' positions were used to collect the acoustic PD signals during the experiment. Each combination consisted of the positions for the 4 AE sensors, which were attached to the surface of the tank wall via magnetic holders. The various combinations were designed to ensure full coverage of the test tank's surface area. The AE sensors' position combinations are provided in Table 1.

Table 1
Examples of AE sensors' position combinations

| Combination | AE Sensor | Sensor Position (cm) | | |
|-------------|-----------|----------------------|----|----|
| | | x | y | z |
| 1 | Sensor 1 | 0 | 15 | 5 |
| | Sensor 2 | 40 | 15 | 20 |
| | Sensor 3 | 5 | 15 | 25 |
| | Sensor 4 | 10 | 10 | 25 |
| 2 | Sensor 1 | 0 | 10 | 5 |
| | Sensor 2 | 40 | 10 | 20 |
| | Sensor 3 | 5 | 10 | 25 |
| | Sensor 4 | 40 | 5 | 10 |
| 3 | Sensor 1 | 0 | 15 | 10 |
| | Sensor 2 | 10 | 15 | 25 |
| | Sensor 3 | 40 | 15 | 15 |
| | Sensor 4 | 0 | 10 | 20 |

Denoising Technique

Once the measured data from the experimental work were acquired, the denoising technique was applied to electrical and acoustic PD signals.

Savitzky-Golay

The Savitzky-Golay (SG) is a time-domain method that performs least-squares polynomial fitting in a specific moving time window. As the time window moves across the input PD signals, a high level of smoothing without significant attenuation and minimal distortion can be generated based on Equation 1.

$$y(i) = \sum_{k=-nL}^{nR} (c_k)(s_{i+k}) \tag{1}$$

In Equation 1, $y(i)$ represents the denoised output for the electrical or acoustic PD signal, while s_{i+k} is the $(i+k)$ -th data point of the corresponding input electrical or acoustic PD signal. The nR and nL indicate the number of data points to the right and left of the current data point, i , respectively. c_k is the SG coefficient obtained from the least squares fitting process (Dombi & Dineva, 2020).

Moving Average

The Moving Average (MA) is a simple denoising method used to denoise a signal by calculating the average magnitude of the data points within a specific window. The MA of a PD signal can be computed based on Equation 2.

$$y(i) = \frac{1}{z} \sum_{k=-\frac{z-1}{2}}^{\frac{z-1}{2}} x(i+k) \tag{2}$$

In Equation 2, $y(i)$ represents the moving average at the i -th data point of the input electrical or acoustic PD signal, and $x(i+k)$ refers to the data points within a window of size z centered around the current data point $x(i)$.

Denoising Evaluation

SNR was utilized based on the equation in Yang et al. (2022) to assess the performance of the denoising methods. To assess the distortion of the waveforms for the denoised signal in comparison to the original signal, RMSE was employed based on the equation in Chaudhuri et al. (2023). The similarity of the denoised and original signals was evaluated using the correlation coefficient (CC) through the equation in Javandel et al. (2022).

PD Source Localization

In this study, the electrical PD signal served as the reference for acoustic PD signal detection for time of arrival calculation. This reference signal was crucial for synchronizing the acoustic PD signal to calculate the time delay. The PD source localization was subsequently performed using both time of arrival and TDOA, as outlined in Equation 3 (Ghosh et al., 2017; Sinaga et al., 2012). In this setup, sensor 2 was set as the reference sensor.

$$\begin{bmatrix} x \\ y \\ z \end{bmatrix} = - \begin{bmatrix} x_{12} & y_{12} & z_{12} \\ x_{32} & y_{32} & z_{32} \\ x_{42} & y_{42} & z_{42} \end{bmatrix}^{-1} \times \left\{ \begin{bmatrix} r_{12} \\ r_{32} \\ r_{42} \end{bmatrix} r_2 + \frac{1}{2} \begin{bmatrix} r_{12}^2 - K_1 + K_2 \\ r_{32}^2 - K_3 + K_2 \\ r_{42}^2 - K_4 + K_2 \end{bmatrix} \right\} \quad [3]$$

$$r_2 = \sqrt{[(x - x_2)^2 + (y - y_2)^2 + (z - z_2)^2]} \quad [4]$$

In Equation 3, x , y , and z represent the coordinates of the estimated PD source. The terms x_{j2} , y_{j2} , and z_{j2} jointly refer to the distance between sensor j and the reference sensor, while r_{j2} is the TDOA between sensor j and the reference sensor times the speed of the acoustic PD signal in RBDPO. The variable r_2 denotes the distance between the reference sensor and the estimated PD source, and K_j values are calculated as $K_j = x_j^2 + y_j^2 + z_j^2$. In the experiment, the velocity of the acoustic PD signal in RBDPO was set to 1528.22 ms^{-1} (Ahmad et al., 2023). For Equation 3, all the terms were known values except for r_2 . The x , y , and z coordinates were first expressed as functions of r_2 and then substituted into Equation 4. The positive solution for r_2 obtained from Equation 4 was substituted back into Equation 3 to solve the equation. The x , y , and z coordinates computed from Equation 3 represented the estimated PD source location based on the given positions of the AE sensors and the TDOA obtained from the denoised signals.

The TDOA between any pair of the AE sensors was computed as the difference between the time of arrival of the acoustic PD signal at each sensor. In order to determine the time of arrival of the acoustic PD signal for each of the AE sensors, the first peak method was selected according to Sarathi et al. (2014). The signal was first denoised and then converted to unipolar. Next, the signal was normalized by dividing the magnitude of each data point by the maximum magnitude of the signal. The first peak of the denoised acoustic PD signal that exceeded a pre-defined magnitude threshold was identified as the time of arrival for the particular sensor. Location error analysis was performed to evaluate the accuracy of the estimated PD source locations based on the equation in Kozako et al. (2012).

RESULT AND DISCUSSION

Partial Discharge Characteristic

Electrical Partial Discharge

Figure 4 shows an example of the electrical PD signal acquired at an applied voltage of 35 kV. The pattern of the electrical PD signal is in accordance with the standard IEC 60270 (CIGRE TB 676, 2017).

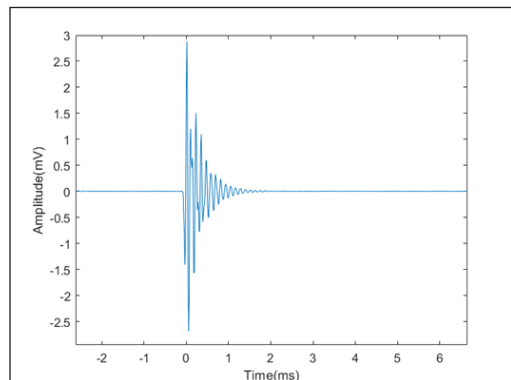


Figure 4. Typical electrical PD signal obtained from the PD experiment

Acoustic Emission Partial Discharge

The examples of acoustic PD signals with strong oil path and strong steel path characteristics can be seen in Figures 5(a) and 5(b), respectively. The contours of the acoustic PD signals are similar to those depicted in (CIGRE TB 676, 2017). The acoustic PD signal in Figure 5(a) propagates through oil over a total distance and time of 30.03 cm and 196.55 μ s. In Figure 5(b), the total distance and time for the acoustic PD signal to propagate along the steel wall are 16.34 cm and 106.94 μ s.

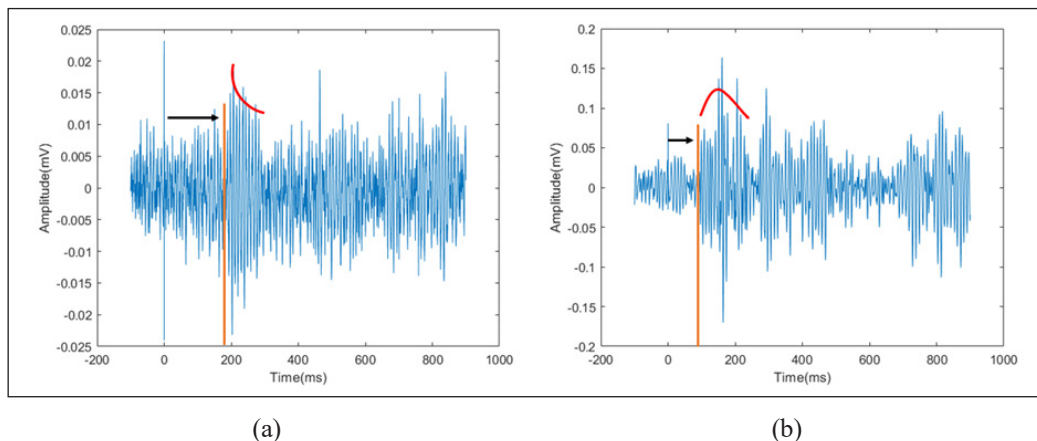


Figure 5. Acoustic PD signal with strong (a) oil and (b) steel path characteristics

Denoising Analysis

The original electrical and acoustic PD signals can be subjected to various kinds of noises such as mechanical noise, white noise and discrete spectral interference (Hashim et al., 2023). Thus, the denoising methods are applied to remove the noise from the original signals. Examples of original and denoised electrical and acoustic PD signals based on SG and MA can be found in Figures 6 and 7. It is shown that SG and MA can remove the reflection of the acoustic PD signal at the origin (Figure 7). As seen in Figure 8(a), while MA effectively smooths the ripples of the electrical PD signal, it also slightly reduces the magnitude of the electrical PD signal. The arrival time for the electrical PD signal using both methods shows almost the same result as the original signal. Although the starting time of SG- and MA-denoised acoustic PD signals is the same as the original signal, the first peak of the acoustic PD signal that is denoised by the MA is delayed by 0.7 μ s from the original signal, whereby it can affect the accuracy of time of arrival measurement, as illustrated in Figure 8(b). The SG can remove the noise and retain the essential characteristics of the original acoustic signal, such as peak and width, including a minor peak, as shown in Figure 8(b), whereby the arrival time is delayed by only 0.1 μ s.

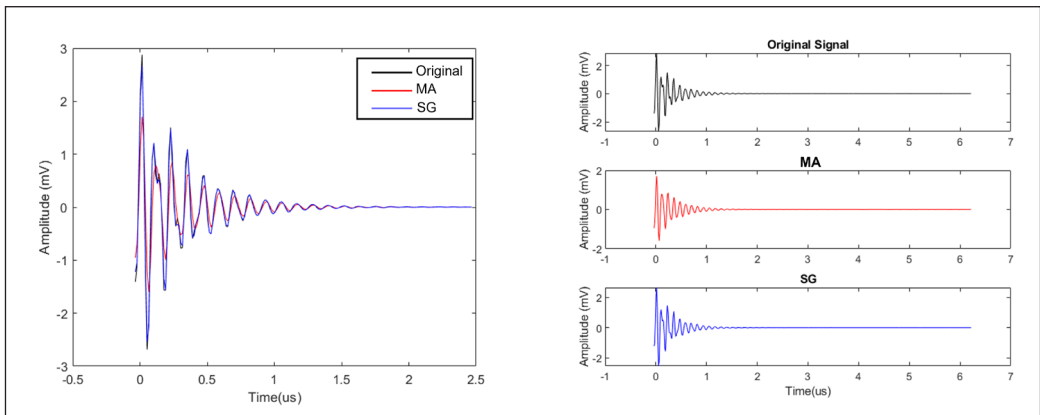


Figure 6. Original and denoised electrical PD signals based on SG and MA

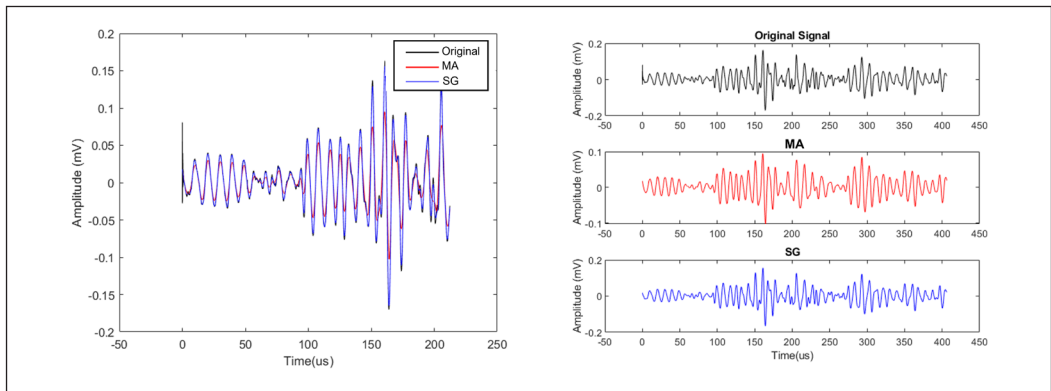


Figure 7. Original and denoised acoustic PD signals based on SG and MA

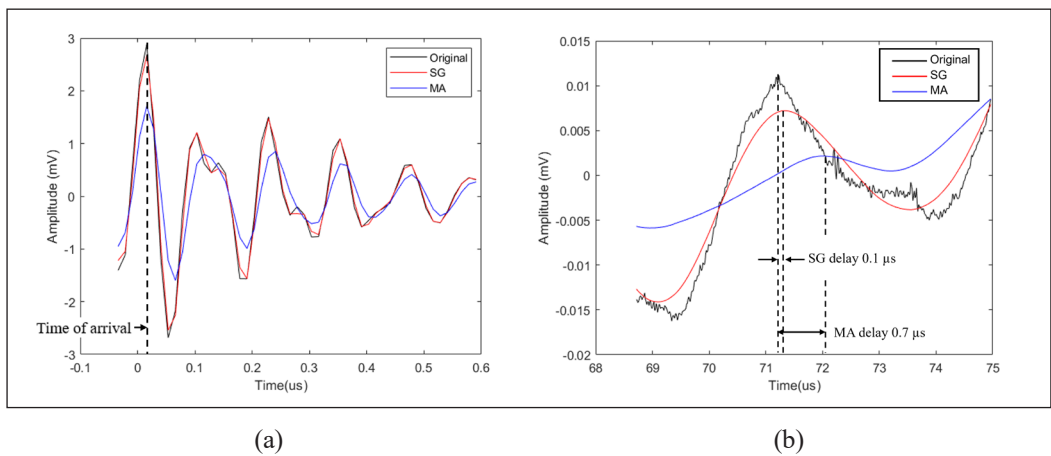


Figure 8. Time of arrival of (a) electrical and (b) acoustic PD signals based on SG and MA denoising methods

The denoising performances for SG and MA for the electrical and acoustic PD signals based on the SNR, RMSE and CC analyses can be seen in Table 2. The SG performs better than MA in denoising the electrical PD signals based on the lower RMSE of 0.1144 and higher CC of 0.9938. Although the MA achieves a higher SNR of 3.8816 than the SG, this may be due to the greater reduction in the magnitude of the MA-denoised signal. The SG also performs better for acoustic PD signals than the MA, as indicated by the low RMSE of 0.0018 and high CC of 0.9746. The high SNR by the MA is possibly due to the significant distortion in the denoised acoustic PD signal, as shown in Figure 8(b).

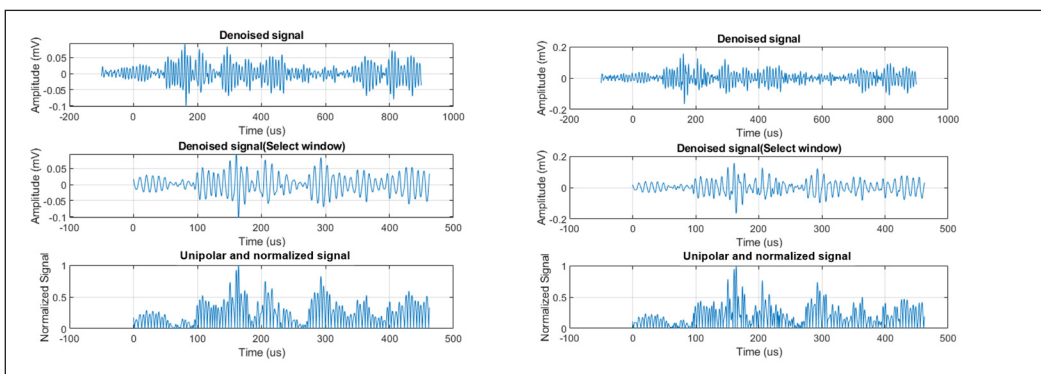
Table 2

Denoising performance of SG and MA based on the SNR, RMSE and CC analyses

| Denoising Method | Signal | SNR | RMSE | CC |
|------------------|---------------|--------|--------|--------|
| Savitzky-Golay | Electrical PD | 0.3222 | 0.1144 | 0.9938 |
| | Acoustic | 1.1016 | 0.0018 | 0.9746 |
| Moving Average | Electrical PD | 3.8816 | 0.5160 | 0.8917 |
| | Acoustic | 6.4177 | 0.0061 | 0.6201 |

Partial Discharge Localization

Figure 9 shows examples of normalized and unipolar acoustic PD signals. The acoustic PD signal denoised by SG yields a higher amplitude than that of MA. The acoustic PD signal that is denoised by MA is smoother than that of SG. Compared to SG, the acoustic PD signal denoised by MA can be easily identified.



(a)

(b)

Figure 9. Unipolar and normalized acoustic PD signal based on (a) SG and (b) MA denoising methods

The 3D model in Figure 10 shows the visual representation of PD localization using both denoising techniques. Table 3 quantitatively compares the estimated and actual PD source locations across the x, y, and z axes for each method. The actual PD source

locations based on SG demonstrate small differences between estimated and actual PD source locations, with differences, Δ of 0.0039 m, 0.0132 m, and 0.0132 m along the x, y, and z axes, respectively. In contrast, the estimated PD source locations based on MA present slightly large differences, particularly along the x and y axes, with 0.0054 m and 0.0175 m, respectively.

Table 3

Comparison of actual PD source location based on SG and MA denoising methods

| Type of filter | SG | | | MA | | |
|----------------------|--------|--------|--------|--------|--------|--------|
| | x (m) | y (m) | z (m) | x (m) | y (m) | z (m) |
| Estimated | 0.0739 | 0.0932 | 0.1668 | 0.0646 | 0.0975 | 0.1745 |
| Actual | 0.07 | 0.08 | 0.18 | 0.07 | 0.08 | 0.18 |
| Difference, Δ | 0.0039 | 0.0132 | 0.0132 | 0.0054 | 0.0175 | 0.0055 |

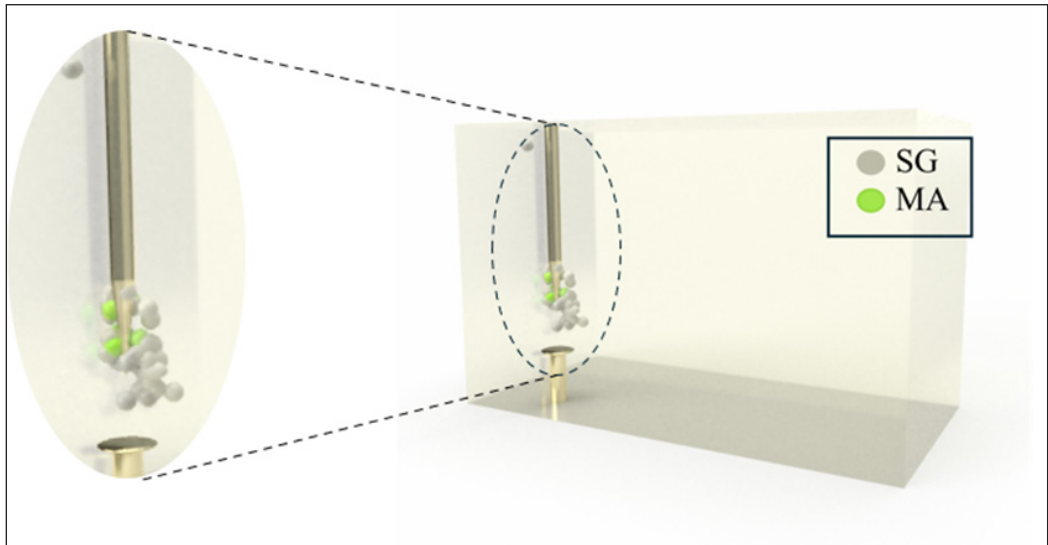


Figure 10. 3D model of PD localization based on SG and MA denoising methods

Table 4 highlights the location error and relative error for both denoising methods. The estimated PD source location based on SG achieves a lower location error of 0.0668 m compared to the MA with 0.0669 m. Although the absolute difference in location error is small, the relative error is slightly lower for SG, with 6.684%, compared to 6.691% for MA. This indicates that while both methods are relatively close in terms of PD localization accuracy in RBDPO, the SG consistently outperforms the MA, particularly in minimizing the deviation from the actual PD source location. The accuracy of the acoustic PD source localization achieved based on the SG-denoised acoustic PD signal in RBDPO is

comparable to that of mineral oil (Hashim et al., 2022). This highlights the ability of SG-denoised signals to improve acoustic PD source localization among different insulating fluids with distinct viscosities.

Table 4

Location error of the estimated PD source location based on SG and MA denoising methods

| Evaluation | SG | MA |
|-----------------------------|-------------|-------------|
| Location relative error (%) | 6.684033005 | 6.691435483 |
| Location error (m) | 0.06684033 | 0.066914355 |

CONCLUSION

It is found that the SG can denoise the electrical and acoustic PD signals better than MA based on SNR, RMSE and CC analyses. The estimated PD source locations based on the denoised PD data by SG are more scattered than those by MA. Nevertheless, the estimated PD source locations at the x and y axes based on the denoised PD data by SG are closer to the actual PD source than those of MA. Future research could explore optimizing the SG parameters to further enhance the PD localization approach. In addition, advanced techniques could be explored for the denoising of electrical and acoustic PD signals and PD localization.

ACKNOWLEDGEMENT

This research was funded by Universiti Putra Malaysia, Inisiatif Putra Berkumpulan GP-IPB (GP-IPB/2022/9717000) funding. Special thanks to Advanced Lightning, Power and Energy Research (ALPER), and UPM for their technical support during this research.

REFERENCES

Ahmad, N. D., Hashim, A. H. M., Azis, N., Talib, M. A., Rezali, K. A. M., Nik Ali, N. H., Jasni, J., Masahiro, K., & Jamil, M. K. M. (2023). Partial discharge localization of refined bleached deodorized palm oil (RBDPO) based on acoustic emission method. In *2023 12th Asia-Pacific International Conference on Lightning (APL)* (pp. 1-5). IEEE. <https://doi.org/10.1109/APL57308.2023.10181667>

Azis, N., Jasni, J., Ab Kadir, M. Z. A., & Mohtar, M. N. (2014). Suitability of palm based oil as dielectric insulating fluid in transformers. *Journal of Electrical Engineering and Technology*, *9*(2), 662–669. <https://doi.org/10.5370/JEET.2014.9.2.662>

Chan, J. Q., Raymond, W. J. K., Illias, H. A., & Othman, M. (2023). Partial discharge localization techniques: A review of recent progress. *Energies*, *16*(6), Article 2863. <https://doi.org/10.3390/en16062863>

Chaudhuri, S., Ghosh, S., Dey, D., Munshi, S., Chatterjee, B., & Dalai, S. (2023). Denoising of partial discharge signal using a hybrid framework of total variation denoising-autoencoder. *Measurement: Journal of the International Measurement Confederation*, *223*, Article 113674. <https://doi.org/10.1016/j.measurement.2023.113674>

- CIGRE TB 676. (2017). *Partial discharges in transformers*. ECIGRÉ. <https://www.e-cigre.org/publications/detail/676-partial-discharges-in-transformers.html>
- Dombi, J., & Dineva, A. (2020). Adaptive savitzky-golay filtering and its applications. *International Journal of Advanced Intelligence Paradigms*, 16(2), 145–156. <https://doi.org/10.1504/IJAIP.2020.107011>
- Feizifar, B., Müller, Z., Fandi, G., & Usta, O. (2019, June). A collective condition monitoring algorithm for on-load tap-changers. In *2019 IEEE International Conference on Environment and Electrical Engineering and 2019 IEEE Industrial and Commercial Power Systems Europe (EEEIC/I&CPS Europe)* (pp. 1-6). IEEE. <https://doi.org/10.1109/EEEIC.2019.8783320>
- Firuzi, K., Vakilian, M., Phung, B. T., & Blackburn, T. R. (2019). Partial discharges pattern recognition of transformer defect model by LBP & HOG features. *IEEE Transactions on Power Delivery*, 34(2), 542–550. <https://doi.org/10.1109/TPWRD.2018.2872820>
- Fuhr, J. (2005). Procedure for identification and localization of dangerous PD sources in power transformers. *IEEE Transactions on Dielectrics and Electrical Insulation*, 12(5), 1005–1014. <https://doi.org/10.1109/TDEI.2005.1522193>
- Ghosh, R., Chatterjee, B., & Dalai, S. (2016, November). A new method for the estimation of time difference of arrival for localization of partial discharge sources using acoustic detection technique. In *2016 IEEE 7th Power India International Conference (PIICON)* (pp. 1-5). IEEE. <https://doi.org/10.1109/POWERI.2016.8077180>
- Guiñón, J. L., Ortega, E., García-Antón, J., & Pérez-herranz, V. (2007, September 3-7). *Moving average and savitzki-golay smoothing filters using mathcad*. [Paper presentation]. International Conference on Engineering Education (ICEE), Coimbra, Portugal.
- Hashim, A. H. M., Azis, N., Jasni, J., Radzi, M. A. M., Kozako, M., Jamil, M. K. M., & Yaakub, Z. (2023). Examination on the denoising methods for electrical and acoustic emission partial discharge signals in oil. *Indonesian Journal of Electrical Engineering and Informatics*, 11(3), 791–804. <https://doi.org/10.52549/ijeei.v11i3.4463>
- Hashim, A. H. M., Azis, N., Jasni, J., Radzi, M. A. M., Kozako, M., Jamil, M. K. M., & Yaakub, Z. (2022). Partial discharge localization in oil through acoustic emission technique utilizing fuzzy logic. *IEEE Transactions on Dielectrics and Electrical Insulation*, 29(2), 623–630. <https://doi.org/10.1109/TDEI.2022.3157911>
- Hussain, M. R., Refaat, S. S., & Abu-Rub, H. (2021). Overview and partial discharge analysis of power transformers: A literature review. *IEEE Access*, 9, 64587–64605. <https://doi.org/10.1109/ACCESS.2021.3075288>
- Javandel, V., Vakilian, M., & Firuzi, K. (2022). Multiple partial discharge sources separation using a method based on laplacian score and correlation coefficient techniques. *Electric Power Systems Research*, 210, Article 108070. <https://doi.org/10.1016/j.eprsr.2022.108070>
- Karami, H., Azadifar, M., Mostajabi, A., Rubinstein, M., Karami, H., Gharehpetian, G. B., & Rachidi, F. (2020). Partial discharge localization using time reversal: Application to power transformers. *Sensors*, 20(5), Article 1419. <https://doi.org/10.3390/s20051419>
- Kozako, M., Murayama, H., Hikita, M., Kashine, K., Nakamura, I., & Koide, H. (2012). New partial discharge location method in power transformer based on acoustic wave propagation characteristics using numerical simulation. In *2012 IEEE International Conference on Condition Monitoring and Diagnosis* (pp. 854–857). IEEE. <https://doi.org/10.1109/CMD.2012.6416284>

- Li, Y., Han, D., Tang, B., Li, K., Qiu, Z., & Zhang, G. (2021). The influence of electrode materials on the emission spectrum in SF₆ under AC corona discharge. In *2021 IEEE Electrical Insulation Conference (EIC)* (pp. 707-710). IEEE. <https://doi.org/10.1109/EIC49891.2021.9612340>
- Lonkwic, P., Szydło, K., & Molski, S. (2017). Savitzky-golay method for the evaluation of deceleration of the friction lift. *Advances in Science and Technology Research Journal*, *11*(1), 138–146. <https://doi.org/10.12913/22998624/68459>
- Mustam, M. M., Azis, N., Jasni, J., Halis, R., Talib, M. A., Yunus, R., Raof, N. A., & Yaakub, Z. (2023). Short-term ageing study on the palm oil and mineral oil in the presence of insulation paper, moisture, low molecular weight acid, and oxygen. *Pertanika Journal of Science and Technology*, *31*(6), 2931–2946. <https://doi.org/10.47836/pjst.31.6.16>
- Pattanadach, N., & Muhr, M. (2017). Comments on PDIV testing procedure according to IEC 61294. In *2017 IEEE 19th International Conference on Dielectric Liquids (ICDL)* (pp. 1-4). IEEE. <https://doi.org/10.1109/ICDL.2017.8124658>
- Purnamasari, D. N., Wibisono, K. A., & Sukri, H. (2021). Digital moving average filter application for echo signals and temperature. *E3S Web of Conferences*, *328*, Article 02007. <https://doi.org/10.1051/e3sconf/202132802007>
- Rafiq, M., Lv, Y. Z., Zhou, Y., Ma, K. B., Wang, W., Li, C. R., & Wang, Q. (2015). Use of vegetable oils as transformer oils-A review. *Renewable and Sustainable Energy Reviews*, *52*, 308–324. <https://doi.org/10.1016/j.rser.2015.07.032>
- Sarathi, R., Sheema, I. P. M., & Subramanian, V. (2014). Effect of barrier in the propagation of partial discharge signals. In *Proceedings of 2014 International Symposium on Electrical Insulating Materials* (pp. 249-252). IEEE. <https://doi.org/10.1109/ISEIM.2014.6870765>
- Seo, J., Ma, H., & Saha, T. K. (2018a). An improved spatial intersectional method for partial discharge (PD) source localization in power transformer. In *2018 12th International Conference on the Properties and Applications of Dielectric Materials (ICPADM)* 363-366. <https://doi.org/10.1109/ICPADM.2018.8401064>
- Seo, J., Ma, H., & Saha, T. K. (2018b). On savitzky – Golay filtering for online condition monitoring of transformer on-load tap changer. *IEEE Transactions on Power Delivery*, *33*(4), 1689–1698. <https://doi.org/10.1109/TPWRD.2017.2749374>
- Sinaga, H. H., Phung, B. T., & Blackburn, T. R. (2012). Partial discharge localization in transformers using UHF detection method. *IEEE Transactions on Dielectrics and Electrical Insulation*, *19*(6), 1891–1900. <https://doi.org/10.1109/TDEI.2012.6396945>
- Yang, J., Yan, K., Wang, Z., & Zheng, X. (2022). A novel denoising method for partial discharge signal based on improved variational mode decomposition. *Energies*, *15*(21), Article 8167. <https://doi.org/10.3390/en15218167>
- Zhang, G., Zhang, X., Tang, J., & Cheng, H. (2018). Study on localization of transformer partial discharge source with planar arrangement UHF sensors based on singular value elimination. *AIP Advances*, *8*(10), Article 105232. <https://doi.org/10.1063/1.5055668>